

Resonance distribution in open quantum chaotic systems

S. Nonnenmacher and E. Schenck

Institut de Physique Théorique, CEA/DSM/IPhT, CEA-Saclay, 91191 Gif-sur-Yvette, France

In order to study the resonance spectra of chaotic cavities subject to some damping (which can be due to absorption or partial reflection at the boundaries), we use a model of damped quantum maps. In the high-frequency limit, the distribution of (quantum) decay rates is shown to cluster near a “typical” value, which is larger than the classical decay rate of the corresponding damped ray dynamics. The speed of this clustering may be quite slow, which could explain why it has not been detected in previous numerical data.

PACS numbers: 05.45.Mt, 03.65.Nk, 42.55.Sa

Recent experimental and theoretical studies have focussed on the dynamics of waves inside quasi-2-dimensional cavities which are “partially open”; this partial opening may be due to various physical phenomena. For instance, an acoustic wave evolving in air or in a metallic slab will lose intensity due to friction and heating. In a microwave cavity, the dissipation mostly occurs at the boundary through ohmic losses. The light propagating inside a dielectric (micro)cavity is partially reflected at the boundary, which can be described as an “effective damping” at the boundary. In all these systems, the discrete stationary modes correspond to complex eigenvalues (or resonances) of the form $k_n = \omega_n - i\Gamma_n/2$, where Γ_n is called the *decay rate* of the mode.

When the shape of the cavity induces a *chaotic* ray dynamics (e.g. the “stadium” shape), the eigenvalues $\{k_n\}$ cannot be computed analytically, but methods of “quantum chaos” can be applied to predict their statistical distribution in the high-frequency limit $\omega_n \rightarrow \infty$. Statistical studies of resonances started in the 1960’ with initial applications to nuclear physics [2]. New applications emerged when experiments on mesoscopic quantum dots [3], microwave cavities [4] or optical fibers [5] allowed to construct cavities with prescribed geometries, and study the dependence of the quantum dynamics with respect to this geometry. A recent interest for dielectric microcavities comes from the potential applications to microlasers: choosing the shape of the cavity appropriately allows to produce a strongly directional emission [6]. The first step to understand the (nonlinear) lasing modes is to study the passive (resonant) modes of the cavity.

Various dissipation effects have been taken into account by adding to the self-adjoint Hamiltonian (representing the dissipationless system) an effective imaginary part, which describes the coupling between the internal cavity modes and the external channels [7]. One analytical tool to study chaotic cavities has been to replace the Hamiltonian (and sometimes also the effective coupling) by some sort of random matrix: this has led to theoretical distributions, which have been favorably compared with numerical or experimental spectra [8, 9].

In this Rapid Communication we focus on situations where the coupling is strongly nonperturbative, and is

distributed over a large part of the cavity or of its boundary, so that the number of coupled channels becomes “macroscopic” in the high-frequency (semiclassical) limit. Using a *nonrandom* model of *damped quantum maps*, we find that, in this limit, the distribution of quantum decay rates becomes asymptotically peaked on a “typical” value γ_{typ} , which is the ergodic mean of the local damping rate. This clustering does not seem to appear if one replaces the unitary part of the quantum map by a *random* unitary matrix, as is often done in the quantum chaos literature [14, 30]. Such a clustering has been rigorously proved for damped waves on ergodic manifolds [15]; we believe it to occur as well in the various types of partially open quantum systems mentioned above. Yet, the width of the distribution may decay very slowly in the semiclassical limit ($\lesssim (\ln k)^{-1/2}$), which could explain why this semiclassical clustering is hardly visible in numerical computations of chaotic dielectric cavities [10, 11, 13] or damped quantum maps [14]; such a slow decay indeed occurs within a solvable toy model we briefly describe at the end of this note.

Let us now describe the model of damped quantum map, which has been introduced and numerically investigated in [14] to mimick the resonance spectra of dielectric microcavities. To motivate this model, we first briefly analyse the dynamics of a few cavity wave systems. The first situation consists in a smooth absorption inside the cavity, represented by the *damped wave equation* $(\partial_t^2 - \Delta + 2b(x)\partial_t)\psi(x, t) = 0$. Here the “damping function” $b(x) \geq 0$ measures the local absorption rate. A high-frequency wavepacket evolving along a classical trajectory is continuously damped by a factor $\approx e^{-\int_0^t b(x(s))ds}$. The classical limit of the dynamics consists in the propagation of rays with decreasing intensity, also called *weighted ray dynamics* (Fig. 1, (a)). When the dissipation occurs at the boundary (e.g. through ohmic losses), an incident high-frequency wavepacket hitting the boundary will be reflected, with its amplitude reduced by a *subunitary* factor $a(q, \varphi)$ (Fig. 1, (b)). The same phenomenon effectively occurs in the case of light scattering through a quasi-2D dielectric microcavity of optical index $n > 1$. The rays propagating inside the

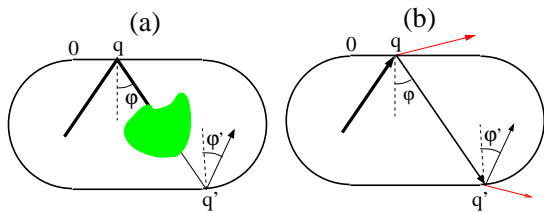


FIG. 1: (a) Weighted ray dynamics inside a cavity with inhomogeneous absorption. (b) absorption (or partial reflection) at the boundary. The ray intensity corresponds to its thickness (color online).

cavity are partially reflected at the boundary, the remaining part being refracted outside and never return provided the cavity is convex. In the high-frequency limit, the reflection factor is given by Fresnel's coefficient, which depends on the light polarization and of $p = \sin \varphi$. For instance, in case of transverse magnetic polarization, the coefficient is a simple complex function $a_{TM}(p)$ [14], which has unit modulus when $|p| \geq 1/n$ (full reflection) and is minimal at $a_{TM}(0) = \frac{n-1}{n+1}$.

To analyze a 2D classical billiard, it is convenient to reduce the flow to the *bounce map* $\kappa : (q, p = \sin \varphi) \mapsto (q', p' = \sin \varphi')$, which acts canonically on the boundary phase space. At the quantum level, the spectrum of the closed cavity can be obtained by studying a k -dependent integral operator acting on the boundary, which effectively quantizes the bounce map, with an effective Planck's constant $\hbar_{eff} = k^{-1}$ [16].

This observation leads to consider canonical maps κ on simple 2-dimensional phase spaces, and quantize them into unitary propagators (*quantum maps*) $U_N(\kappa)$ of finite dimension $N \sim \hbar_{eff}^{-1}$ [17]. A Gaussian wavepacket $|q, p\rangle$ localized at the phase space point (q, p) is first transformed unitarily into a deformed wavepacket $U_N |q, p\rangle$, localized near $\kappa(q, p)$. To induce some damping, we then multiply this state by a factor $a(\kappa(q, p))$, which can be implemented by applying to $U_N |q, p\rangle$ the operator $\text{Op}_N(a)$ quantizing the damping factor. The latter is generally complex-valued, we will assume that it satisfies the following bounds:

$$\forall q, p, \quad 0 < a_{\min} \leq |a(q, p)| \leq a_{\max} = 1. \quad (1)$$

These two steps lead to the definition of the *damped quantum map*

$$M_N = M_N(a, \kappa) = \text{Op}_N(a) \circ U_N(\kappa).$$

The classical limit of the dynamics generated by M_N acts on “weighted point particles”: a point at position (q, p) is moved to $\kappa(q, p)$ and its weight is reduced by a factor $|a(\kappa(q, p))|^2$. This is the discrete-time version of a weighted ray dynamics. Compared with cavity systems, this model has two main advantages: one can easily engineer a map κ with specific dynamical properties; the

spectrum of $M_N(a, \kappa)$ is easier to study both numerically and analytically.

The spectrum $\{\lambda_j^{(N)}, j = 1, \dots, N\}$ of $M_N(a, \kappa)$ is the main object of our study (eigenvalues are ordered by decreasing moduli). To compare it with the resonance spectrum of a damped cavity, one should extract from the latter an interval $\{|\omega_n - k| \leq \pi\}$ around the frequency $k \sim N$. The distribution of the decay rates $\{\Gamma_n : |\omega_n - k| \leq \pi\}$ should parallel that of the decay rates $\{\gamma_j^{(N)} = -2 \ln |\lambda_j^{(N)}|, j = 1, \dots, N\}$.

A similar model had been introduced in [19, 20] to mimic “fully open” cavities: the damping factor $a(z)$ was then vanishing inside the opening. Such systems were characterized by a *fractal Weyl law* [18, 19, 20]: the number of resonances in a strip $\{\omega_n \leq k, \Gamma_n \leq \Gamma\}$ grew like $k^{1+\delta}$, where $\delta < 1$ was given by the fractal dimension of the trapped set. On the opposite, the bounds (1) imply that for N large enough, M_N is invertible, and its N eigenvalues are contained inside the annulus $\{a_{\min} \leq |\lambda_j^{(N)}| \leq 1\}$. Transposed to the case of an absorbing cavity, it implies that all high-frequency resonances are contained in a fixed strip $\{\Gamma_n \leq \Gamma_{\max}\}$, and the number of modes $\#\{k_n, |\omega_n| \leq k\}$ asymptotically grows like $C k^2$, thus satisfying a *standard Weyl law* [15]. The situation is more complicated for dielectric cavities. Explicit solutions in the case of the circular cavity [12] suggest that resonances split between two well-separated groups: “inner” resonances contained in a strip $\{\Gamma_n \leq \Gamma\}$, and “outer” resonances $\Gamma_n \sim \omega_n^{1/3}$ associated with modes localized outside the cavity. Since our damped quantum map only acts on states localized “inside the torus”, we believe that the above Weyl asymptotics correctly counts the inner resonances of dielectric cavities (the fractal Weyl law recently observed in [13] is probably a finite-frequency artifact).

To obtain a more precise description, one needs to iterate the dynamics, that is study the time- n evolution M_N^n . Applying the quantum-classical correspondence (“Egorov's theorem”), we find that

$$(M_N(a, \kappa)^{n\dagger} M_N(a, \kappa)^n)^{1/2n} \approx \text{Op}_N(a_n), \quad (2)$$

where the function $a_n = (\prod_{i=1}^n |a \circ \kappa^i|)^{1/n}$ is the average damping over trajectory stretches of length n . The approximation is valid in the semiclassical limit $N \rightarrow \infty$.

Much can be drawn from the knowledge of the functions $-2 \ln a_n$ in the long-time limit $n \gg 1$. Their *ranges* consist in intervals $I_n(a) \subset I_{n-1}(a)$, which converge to a limit interval $I_\infty(a)$ when $n \rightarrow \infty$. The above identity implies that the quantum decay rates $\gamma_j^{(N)}$ must be contained in $I_\infty(a)$ for large enough N [15]. Numerical [14] and analytical [21] studies indicate that the “quantum ranges” $J_N(a) = [\gamma_1^{(N)}, \gamma_N^{(N)}]$ generally remain strictly inside $I_\infty(a)$, in particular stay at finite distance from

zero. Adapting methods used to study scattering systems [23, 24], one finds that high-frequency decay rates should be larger than $\gamma_{gap} \stackrel{\text{def}}{=} -2\mathcal{P}_\kappa(\ln|a| - \lambda^u/2)$, where $\mathcal{P}_\kappa(\cdot)$ is the *topological pressure* associated with the map κ and the observable $(\ln|a| - \lambda^u/2)$ [25], $\lambda^u(z)$ being the expansion rate of κ along the unstable direction. The lower bound γ_{gap} may be trivial (negative) when $|a(z)|$ varies little across the phase space (see the last line in Table I).

Since κ is chaotic, the *value distribution* of $-2\ln a_n(z)$ becomes peaked around its average $\gamma_{typ} = -2 \int \ln|a(z)| dz$ when $n \rightarrow \infty$. The central limit theorem [26] shows that this distribution is asymptotically a Gaussian of width $\frac{\sigma(a)}{\sqrt{n}}$ around γ_{typ} . This distribution is semiclassically connected with the spectral density of $\text{Op}_N(a_n)$:

$$\#\{\lambda \in \text{Spec}(\text{Op}_N(a_n)) : \lambda \leq s\} \approx N \text{Prob}(a_n \leq s). \quad (3)$$

From (2), the LHS approximately counts the *singular values* of the matrix M_N^n . Using the Weyl inequalities [27], we obtain that most of the decay rates $\{\gamma_j^{(N)}\}_{j=1,\dots,N}$ satisfy $\gamma_j^{(N)} \geq \gamma_{typ} - \epsilon$.

Applying the same argument to the inverse quantum map $M_N^{-1} \approx M_N(a^{-1} \circ \kappa, \kappa^{-1})$, we eventually find that in the semiclassical limit, most decay rates cluster around γ_{typ} , which we thus call the *typical decay rate*. More precisely, the fraction of the decay rates $\{\gamma_j^{(N)}\}$ which are not in the interval $[\gamma_{typ} - \epsilon, \gamma_{typ} + \epsilon]$ goes to zero when $N \rightarrow \infty$.

By pushing the quantum-classical correspondence up to its limit, namely the *Ehrenfest time* $n \sim C \ln N$, we find that the *width* of the decay rate distribution is at most of order $(\ln N)^{-1/2}$ (a rigorous proof will be given in [28]). Our numerics (see Fig.3) are compatible with this upper bound. Such a slow decay could explain why this concentration has not been detected in previous studies. For a solvable toy model presented at the end of this note, the distribution will be shown to be indeed a Gaussian of width $\sim C(\ln N)^{-1/2}$.

Let us compare the quantum decay rates with the “classical decay rate” γ_{cl} of the corresponding weighted dynamics. The latter, introduced in [22] in the framework of dielectric microcavities, is obtained by evolving an initial smooth distribution of points through the weighted dynamics: for large times n , the total weight of the distribution decays like $W e^{-n\gamma_{cl}}$. As in the case of fully open systems [23], γ_{cl} can be expressed as the topological pressure $\gamma_{cl} = -\mathcal{P}_\kappa(2 \ln|a| - \lambda^u)$. Convexity properties of the pressure allow to compare this classical decay rate with the two rates obtained above: $\gamma_{gap} \leq \gamma_{cl} \leq \gamma_{typ}$, and the inequalities are generally strict (see table I). The quantum ranges $J_N(a)$ may or may not contain the classical rate γ_{cl} (see Fig. 2).

The map we consider in our numerics is the 3-baker’s

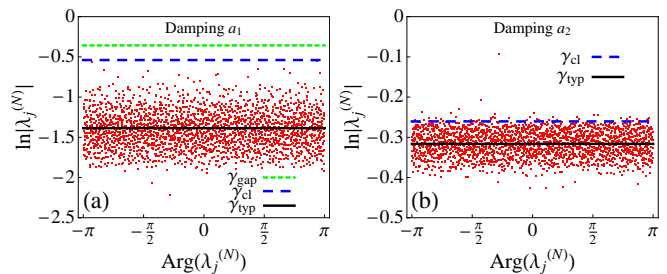


FIG. 2: Spectra of $M_N(\kappa_{bak}, a_i)$ for $N = 2100$ and damping factors a_1 (a) and a_2 (b). We plot $\{i \ln(\lambda_j^{(N)})\}$ to mimick the spectrum of a damped cavity near $k \sim N$ (the vertical coordinates correspond to $-\gamma_j^{(N)}/2$). The horizontal lines indicate $-\gamma_*/2$ for the theoretical rates given in table I.

	γ_{gap}	γ_{cl}	γ_{typ}
a_1	0.715	1.079	2.774
\tilde{a}_1	0.734	1.079	3.070
a_2	-0.523	0.521	0.633

TABLE I: Values of the theoretical rates for κ_{bak} and the various damping functions we use.

map, which acts canonically on the 2-dimensional torus $\{(q, p) \in [0, 1]^2\}$. It is given by $\kappa(q, p) = (3q \bmod 1, \frac{p+3q}{3})$, and generates a strongly chaotic dynamics. This map is quantized as in [29], into a sequence of unitary matrices $U_N = G_N^{-1} \begin{pmatrix} G_{N/3} & & \\ & G_{N/3} & \\ & & G_{N/3} \end{pmatrix}$, where

$(G_M)_{jk} = \frac{1}{\sqrt{M}} \exp(-\frac{2i\pi}{M}(j + \frac{1}{2})(k + \frac{1}{2}))$ is the “symmetrized” discrete Fourier transform. We choose damping factors of the form $a(q)$, so their quantizations $\text{Op}_N(a)$ are simply diagonal matrices with entries $a((j + 1/2)/N)$. The factor $a_1(q)$ has a plateau $a_1(q) \equiv 1$ for $q \in [1/3, 2/3]$, another one $a_1(q) \equiv 0.1$ for $q \in [0, 1/6] \cup [5/6, 1]$, and varies smoothly inbetween. It approximates the piecewise constant function $\tilde{a}_1(q)$ which takes values 0.1, 1, and 0.1 respectively on the intervals $[0, 1/3]$, $[1/3, 2/3]$ and $[2/3, 1]$. Our second choice is the “smoother” function $a_2(q) = 1 - \sin(2\pi q)^2/2$. Since we use a single map κ , the damped quantum maps will be abbreviated by $M_N(a_i)$.

We first notice that all these factors reach their extremal values a_{\min} , a_{\max} on the fixed points $(0, 0)$ and $(1/2, 1/2)$ of κ . As a result, for each of them the asymptotic range $I_\infty(a)$ is equal to $[a_{\min}, a_{\max}]$. The theoretical rates γ_{gap} , γ_{cl} and γ_{typ} for these three factors are given in Table I. In Fig.2 we plot the spectra of $M_N(a_i)$ for $N = 2100$ (the theoretical bound γ_{gap} for a_2 is negative, hence irrelevant). We check that all quantum rates are larger than γ_{gap} . In the case of $M_N(a_1)$, all quantum rates are also larger than γ_{cl} , while $M_N(a_2)$ admits a few smaller decay rates.

The clustering of decay rates around γ_{typ} is already perceptible in Fig.2. To make it more quantitative, in Fig.3 (a) we plot the cumulative distributions of decay rates. At first glance, the widths of the distributions around γ_{typ} seem to depend little on N . Enlarging the set of data, we plot these widths on Fig.3 (b). They indeed decay with N . The 2-parameter power-law fits $A' N^{-B'}$ lead to small exponents B' , which seem to favor the logarithmic fits $A (\ln N)^{-B}$: the latter decay slightly faster than the theoretical upper bound $(\ln N)^{-1/2}$.

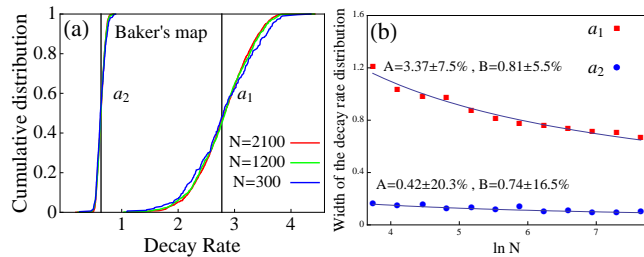


FIG. 3: (a) Cumulative decay rate distribution for $M_N(\kappa, a_i)$. The vertical bars indicate the rates γ_{typ} . (b) Widths of the decay rate distributions, together with the best 2-parameter fits $A (\ln N)^{-B}$ and the asymptotic standard errors. The power-law fits $A' N^{-B'}$ yield $A' = 1.35 \pm 5\%$, $B' = 0.09 \pm 8\%$ for $M_N(a_1)$ and $A' = 0.2 \pm 18\%$, $B' = 0.10 \pm 26.5\%$ for $M_N(a_2)$.

It is possible to construct a *solvable* quantization of the baker's map by taking the quantum parameter $N = 3^k$, $k \in \mathbb{N}$, and replacing the discrete Fourier transform G_N by the Walsh transform [20]. If we then select a damping factor which, like \tilde{a}_1 , takes constant values a^j on the intervals $q \in [j/3, (j+1)/3)$, the quantum model remains solvable. The spectrum of M_N relies on the eigenvalues $\{\lambda_i\}$ of the 3×3 matrix $\text{diag}(a^j)G_3^{-1}$. Taking $\gamma_i = -2 \ln |\lambda_i|$, the N quantum decay rates can be indexed by the sequences $\boldsymbol{\eta} = \eta_1 \eta_2 \dots \eta_k$, with $\eta_i \in \{1, 2, 3\}$: they are given by $\gamma_{\boldsymbol{\eta}} = \frac{1}{k} \sum_{m=1}^k \gamma_{\eta_m}$. For instance, in the case of the damping function \tilde{a}_1 , the rates γ_i take the values (0.803, 3.801, 4.605). From this explicit expression, one easily draws that, in the limit $k \rightarrow \infty$, the distribution of the $\{\gamma_{\boldsymbol{\eta}}\}$ converges to a Gaussian of average $\gamma_{typ} = (\sum_{i=1}^3 \gamma_i)/3$ and variance $\frac{1}{3k} \sum_{i=1}^3 (\gamma_i - \gamma_{typ})^2 = C (\ln N)^{-1/2}$.

To summarize, we have studied the spectra and eigenmodes of damped quantum chaotic maps, a toy model for various types of partially open quantized chaotic cavities, in a régime where the damping is both macroscopic and strongly nonperturbative. We have shown that the quantum decay rates remain inside a fixed interval, and that most of them cluster around the mean damping rate γ_{typ} .

These statistical properties seem to differ from those of non-hermitian random matrices used to represent such open systems.

Acknowledgements: This work was partially supported by the grant ANR-05-JCJC-0107-01. We have benefited from discussions with F.Faure and Y.Fyodorov, and thank E.Bogomolny and R.Dubertrand for sharing their results prior to publication.

-
- [1] R. Weaver, J. Acoust. Soc. Am. **85** 1005 (1989)
 - [2] P.A. Moldauer, Phys. Rev. **171** 1164 (1968)
 - [3] R.A. Jalabert *et al.*, Phys. Rev. Lett. **65** 2442 (1990)
 - [4] U. Kuhl *et al.*, J. Phys. **A 38** 10433 (2005)
 - [5] V. Doya *et al.*, Phys. Rev. Lett. **88** 014102 (2001)
 - [6] C. Gmachl *et al.*, Science **280** 1556 (1998)
 - [7] C.H. Lewenkopf and H.-A. Weidenmüller, Ann. Phys. (NY) **212** 53 (1991)
 - [8] Y.V. Fyodorov and H.-J. Sommers, J. Phys. **A 36** 3303 (2003)
 - [9] T. Kottos, J.Phys. **A 38** 10761 (2005)
 - [10] M. Levental *et al.*, Phys. Rev. **A 75** 033806 (2007)
 - [11] S. Shinohara and T. Harayama, Phys. Rev. **E 75**, 036216 (2007)
 - [12] R. Dubertrand *et al.*, Phys. Rev. **A 77** 013804 (2008); E. Bogomolny *et al.*, arXiv:0807.2374
 - [13] J. Wiersig and J. Main, Phys. Rev. **E 77** 036205 (2008)
 - [14] J.P. Keating *et al.*, Phys. Rev. **A 77** 013834 (2008)
 - [15] J. Sjöstrand, Publ. RIMS **36** 573 (2000)
 - [16] J.-M. Tualle and A. Voros, Chaos, Solitons and Fractals **5**, 1085 (1995)
 - [17] M. Degli Esposti and S. Graffi (eds.), *The mathematical aspects of quantum maps*, Springer, Berlin, 2003
 - [18] W. Lu *et al.*, Phys. Rev. Lett. **91** 154101 (2003)
 - [19] H. Schomerus and J. Tworzydło, Phys. Rev. Lett. **93** 154102 (2004)
 - [20] S. Nonnenmacher and M. Zworski, J. Phys. **A 38**, 10683 (2005); *ibid.*,
 - [21] M. Asch and G. Lebeau, Experimental math. **12** 227 (2003)
 - [22] S.-Y. Lee *et al.*, Phys. Rev. Lett **93** 164102 (2004);
 - [23] P. Gaspard and S.A. Rice, J. Chem. Phys. **90**(1989), 2242
 - [24] M. Ikawa, Ann. Inst. Fourier, **38** (1988), 113 ; S. Nonnenmacher and M. Zworski, arXiv:0706.3242
 - [25] P. Walters, *An introduction to ergodic theory*, Springer, Berlin, 1982
 - [26] M. Ratner, Israel J. Math **16** 181 (1973)
 - [27] Assume the singular values $\{s_i\}$ and eigenvalues $\{\lambda_i\}$ of a $N \times N$ matrix are ordered by decreasing moduli. Then, for any $t > 0$ and any $j \leq N$, one has $\sum_{i=1}^j |\lambda_i|^t \leq \sum_{i=1}^j s_i^t$.
 - [28] E. Schenck, *Weyl law for partially open quantum maps*, in preparation.
 - [29] M.Saraceno, Ann. Phys. (NY) **199** 37 (1990)
 - [30] Y.Weï and Y.V.Fyodorov, arXiv:0809.2726